PTEP

Prog. Theor. Exp. Phys. **2012**, 03C009 (16 pages)
DOI: 10.1093/ptep/pts060

The rare-RI ring

A. Ozawa[1,*], T. Uesaka[2] and M. Wakasugi[2], the Rare-RI Ring Collaboration

[1]*Institute of Physics, University of Tsukuba, Ibaraki 305-8571, Japan*
[2]*RIKEN Nishina Center, Wako, Saitama 351-0198, Japan*
*E-mail: ozawa@tac.tsukuba.ac.jp

Received September 1, 2012; Accepted November 6, 2012; Published December 17, 2012

We describe the rare-RI (radioactive isotope) ring at the RI Beam Factory (RIBF). The main purpose of the rare-RI ring is to measure the mass of very neutron-rich nuclei, the production rates of which are very small (hence 'rare RI') and the lifetimes of which are predicted to be very short. In the rare-RI ring, there are two innovative pieces of apparatus: individual injection, which can realize the injection of 200 A MeV rare RIs one by one, and a cyclotron-like storage ring, which allows high isochronous magnetic fields with large angular and momentum acceptances. With these devices, we will achieve a 10^{-6} mass resolution, and will be able to access rare RIs, the production rate of which is down to 1 event/day/pnA. Construction of the rare-RI ring started in fiscal year 2012.

1. Introduction

The r-process nucleosynthesis is considered to be the origin of about half of all elements heavier than iron observed in nature. Although the r-process is mandatory for the existence of heavy elements, it is not yet clarified where and how it has occurred in the cosmos. What complicates the r-process is two "unknowns": one involves environmental conditions, i.e. temperature, neutron-flux, entropy, under which the r-process has taken place. It is widely accepted that thermal processes cannot be responsible for the r-process, and that *some* radical environment is necessary. At present, type-II supernova explosions and neutron mergers are considered to be strong candidates for the r-process site. The other unknown is the properties of neutron-rich nuclei. The r-process is considered to proceed along a path that is located far from the stability line. In Fig. 1, an "example" of the r-process path prediction, which is estimated based on the KTUY mass formula [1], is shown with a blue line. Black and gray squares indicate stable nuclei and nuclei with known masses cited from AME2011 [2]. It should be noted here that new isotopes along the r-process path prediction have been successfully produced at RIBF very recently [3,4]. The exact location of the r-process path depends strongly on the properties of neutron-rich nuclei, of which very few have so far been produced; this makes theoretical prediction of the path location very difficult. The relevant nuclear properties are mass, beta-decay lifetime, neutron-capture, and photodisintegration rates, but nuclear mass is of primary importance among these [5]. It is obvious that a mass measurement for the r-process region is the best way to proceed in revealing the astrophysical origin of the r-process.

There are some difficulties in measuring the masses of r-process nuclei. Firstly, the production rates of the nuclei are very low. Since the nuclei are located very far from the stability line, the production

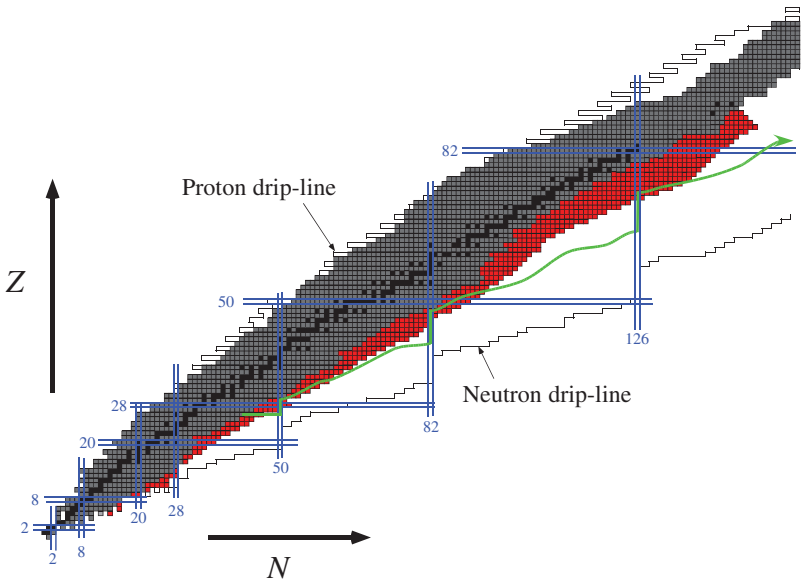

Fig. 1. Nuclear chart for the rare-RI ring. Black squares show stable nuclei and gray squares show nuclei with known masses in AME2011 [2]. Red squares represent nuclei where the beam intensity is more than 1 event/day/pnA in the rare-RI ring. The r-process path estimated by the mass formula KTYU [1] is shown by the green line, and the traditional magic number is shown in blue with numbers.

rate is sometimes as small as $\sim$1 event/day. They are actually "*rare RIs*".This means that we cannot accumulate many events to improve the precision of the measured mass, and thus a device that has an intrinsic mass resolution of 10^{-6} is required. Secondly, the lifetimes of the nuclei are very short, typically less than 50 ms. Thus, we have to measure the mass of the nuclei at small intensity (about 1 event/day) and in a short period of time (less than 50 ms). Although various experimental techniques have been applied to measure nuclear masses so far [6], there are only three techniques that meet our requirements. One is based on an ion-trap technique [7]. An advantage of ion-trap-based techniques is that a high mass resolution of better than 10^{-7} is achievable. Although this high resolution is attractive, a long observation time of $\sim$1 s prevents one from applying this technique to the mass measurement of short-lived r-process nuclei. The other two techniques are conducted in storage rings. The first method is Schottky mass spectrometry (SMS), which has been beautifully demonstrated at the ESR, GSI [8], where a high resolution of better than 10^{-6} can be achieved. On the other hand, a long RI cooling time ($\sim$10 s) is needed to cool the beam, which, again, does not meet our requirements. The last method is isochronous mass spectrometry (IMS), where the detection time can be kept very short, typically less than 1 ms. Thus, IMS can serve as a unique mass-measurement method for short-lived nuclei. IMS has been applied at the ESR, but the resolution achieved there is relatively poor ($\sim 10^{-5}$). This is partly because the ESR, being a synchrotron-type storage ring, cannot have a large acceptance with sufficiently good isochronicity. We definitely need a dedicated setup for IMS to extend the mass measurement to r-process nuclei. This is why we propose to construct a new device: the "rare-RI ring", which fulfills the requirements of a high mass resolution of 10^{-6}, a short measurement time of less than 50 ms, and a high detection efficiency of $\sim$100% for rare RI simultaneously.

In this paper, we give an overview of the rare-RI ring and its mass measurements. In Sect. 2, we describe the principle of mass measurements. In Sect. 3, we introduce the characteristic and design of the apparatus in the rare-RI ring. In Sect. 4, a possible scheme for mass measurements is presented.

In Sect. 5, we present other possible applications other than mass measurements. In Sect. 6, we summarize this paper.

2. Principle of mass measurements

In this section, we present the principle of mass measurements in the rare-RI ring. We start from the cyclotron frequency in the ring. The frequency in the storage ring can be given by the so-called cyclotron frequency (f_c) as

$$f_c = \frac{1}{2\pi}\frac{qB}{m} \tag{1}$$

where m/q is the mass-to-charge ratio of a particle in the ring, and B is the magnetic field of the ring. Thus, the circulation time in the ring (T) is obtained by reversing Eq. (1):

$$T = 2\pi\frac{m}{q}\cdot\frac{1}{B} = 2\pi\frac{m_0}{q}\cdot\frac{1}{B}\cdot\gamma, \tag{2}$$

where $\gamma = 1/\sqrt{1-\beta^2}$, $\beta = v/c$, and c is the light velocity. In an isochronous ring, B becomes $B_0\gamma$ at a certain m_0/q. Thus, we obtain the following equation for a certain m_0/q:

$$T = 2\pi\frac{m}{q}\cdot\frac{1}{B} = 2\pi\frac{m_0}{q}\cdot\frac{1}{B}. \tag{3}$$

We can therefore show that we can determine the mass (more exactly m_0/q) by measuring both T_0 and B_0 accurately. It is noted that T_0 is independent of the kinetic energy of the particle. The relative uncertainty of m_0/q is given by

$$\frac{\delta(m_0/q)}{m_0/q} = \frac{\delta T_0}{T_0} + \frac{\delta B_0}{B_0}. \tag{4}$$

If we measure T_0 and B_0 with an accuracy of order 10^{-6}, we can determine the mass with an accuracy of order 10^{-6}. In reality, however, it is very difficult to maintain the magnetic field strength to be stable within a range of 10^{-6}. Thus, we measure the masses of several nuclei, including nuclei whose masses are well known, at the same time, and deduce the masses of nuclei of interest by using the known masses as references.

For RI beams with different mass-to-charge ratios ($(m_1/q) = m_0/q + \delta(m_0/q)$), isochronism is not fulfilled. In IMS, the orbital of the beam is determined by its rigidity. Thus, if the beams with m_1/q have the same rigidity as that with m_0/q, the circumference is identical and the following equations are fulfilled:

$$\frac{m_0}{q}\gamma_0\beta_0 = \frac{m_1}{q}\gamma_1\beta_1 \tag{5}$$

$$\beta_1 T_1 = \beta_0 T_0 \tag{6}$$

where T_1 and β_1 are the circulation time and the velocity of the nuclei with m_1/q and $\gamma_1 = 1/\sqrt{1-\beta_1^2}$. By using Eq. (5) and (6) the mass-to-charge ratio (m_1/q) can be given by

$$\frac{m_1}{q} = \left(\frac{m_0}{q}\right)\frac{T_1}{T_0}\frac{\gamma_1}{\gamma_0} = \left(\frac{m_0}{q}\right)\frac{T_1}{T_0}\sqrt{\frac{1-\beta_1^2}{1-\left(\frac{T_1}{T_0}\beta_1\right)^2}}. \tag{7}$$

Thus, to evaluate the mass of nuclei with non-isochronism, we need a correction of the velocity (β). The relative differential of m_1/q is given by

$$\frac{\delta(m_1/q)}{m_1/q} = \frac{\delta(m_0/q)}{m_0/q} + \gamma_0^2 \frac{\delta(T_1/T_0)}{T_1/T_0} + k\frac{\delta\beta_1}{\beta_1}, \tag{8}$$

$$k = -\frac{\beta_1^2}{1-\beta_1^2} + \left(\frac{T_1}{T_0}\right)^2 \frac{\beta_1^2}{1-(T_1/T_0)^2\beta_1^2}. \tag{9}$$

The resolution of the mass depends on the resolution of the velocity. If we require an order of 10^{-6} mass resolution, the third term in Eq. (8) should be less than 10^{-6}. A 10^{-2} difference of the mass (i.e., $\delta(m_0/q)/(m_0/q) \sim 10^{-2}$) corresponds to a difference of $\sim 10^{-2}$ in the circulation time and $k \sim 10^{-2}$. Thus, if we determine the velocity with 10^{-4}, the third term in Eq. (8) becomes around 10^{-6}. In summary, for RI beams with non-isochronism we can use Eq. (7) to determine the mass. In the rare-RI ring, it is essential that T_0 and B_0 are less than 10^{-6}, and β is less than 10^{-4}. To achieve these numbers, we designed the storage ring and injection line as described in the next section.

3. Experimental apparatus

The rare-RI ring consists of a cyclotron-like storage ring specialized for isochronous mass spectroscopy of rare RI beams and a long injection line, which is necessary for individual injection and measurement of β with 10^{-4} resolution. The beam energy of the rare-RI ring is designed to be 200 A MeV. The "cyclotron-like" storage ring can achieve the isochronous condition for large acceptances of $\delta x' = \pm 15$ mrad and $\delta p/p = \pm 0.5\%$. The results of early design work are reported in Refs. [9–11]. In this section, we introduce the design concept for the cyclotron-like storage ring, and the characteristics of key pieces of apparatus (individual injection, the long injection line, and detectors) in detail. The basic design values and the layout and location of the rare-RI ring are given in Table 1 and Fig. 2.

3.1 Cyclotron-like storage ring

The storage ring consists of 24 dipole magnets: 4 dipole magnets form one sector and 6 sectors make up the ring. The ring has 6 straight sections and no focusing magnet. The dipole magnets to be used were originally used in a heavy-ion storage ring, TARN-II, at the Institute of Nuclear Study, University of Tokyo [12]. Each dipole magnet causes 15-degree bending with a bending radius of 4.045 m. The gap of each dipole magnet is 80 mm. Both the entrance and exit edges are tilted

Table 1. Basic characteristics of the cyclotron-like storage ring.

Beam energy	200 A MeV
Lorentz factor	1.2147
Circumference	60.3507 m
Momentum acceptance	$\pm 0.5\%$
Revolution frequency	2.82 MHz
Revolution time	355 ns
Betatron tune	$Q_x = 1.25$, $Q_y = 0.84$
Dispersion of straight line	66.9 mm/%

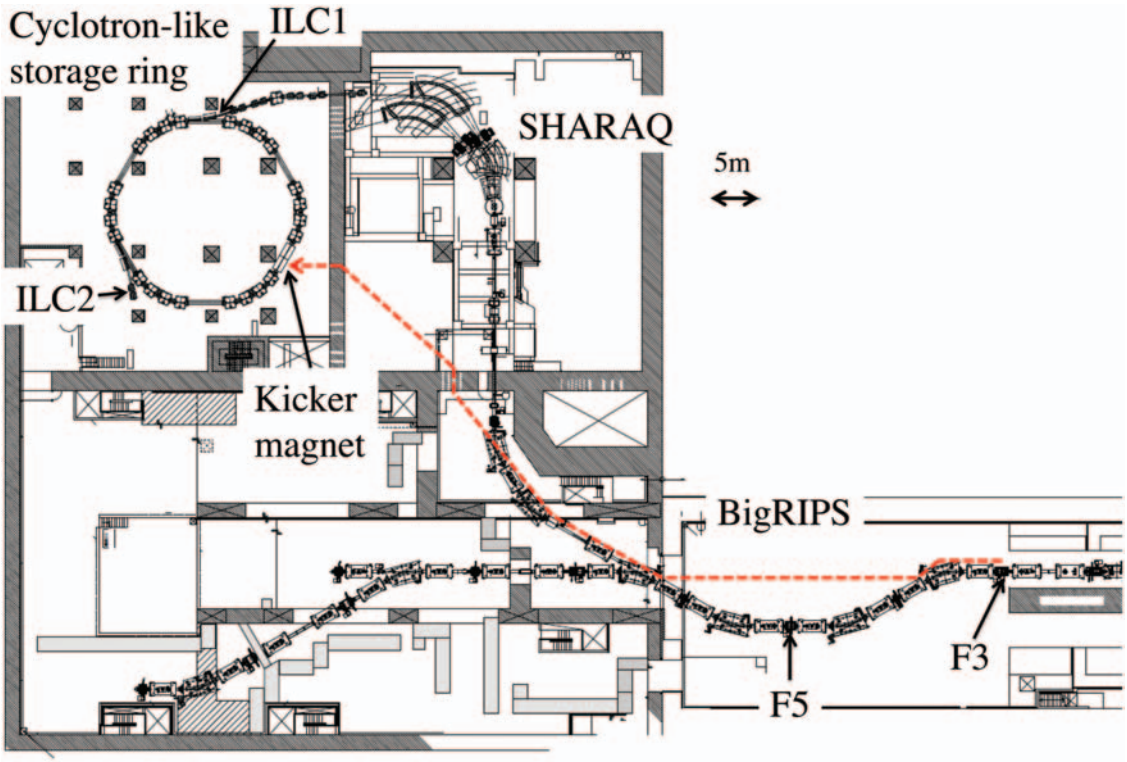

Fig. 2. Layout of the rare-RI ring. The red line shows the path for the high-speed coaxial transmission cable [23], the length of which is ~100 m.

by 7.5 degrees toward the horizontally focusing direction. The circumference of the ring is 60.35 m, which corresponds to a revolution time of 355 ns for rare RI beams with 200 A MeV.

There are two ways of achieving a first-order isochronous field. One is the introduction of edge angles (ε) in the sector magnets; the other is the introduction of an n-value in the sector magnets. In the cyclotron-like storage ring, dispersion matching injection is adopted. Thus, if $n = 0$ (homogeneous magnetic field), to achieve a first-order isochronous field, ε can be given by

$$\tan\varepsilon = \frac{(R\phi + S) - R\phi\gamma^2}{(R\phi + S) - R\phi\gamma^2 + 2R\gamma^2 \tan\phi/2}\tan\phi/2, \tag{10}$$

where R, S, and ϕ are the radius of the central orbit in the magnetic sector, the length of straight section along the central orbit, and the bending angle, respectively [13]. In this case, the dispersion (ξ) is given by

$$\xi = \frac{\tan\phi/2}{\tan\phi/2 - \tan\varepsilon}R. \tag{11}$$

Under dispersion matching injection, an isochronicity of about 3×10^{-5} is achieved over the momentum range from -1% to $+1\%$ in δp. For the case $\varepsilon = 0$, to achieve a first-order isochronous field the n-value is given as follows. From the magnetic rigidity, BR, the relative differential of B is given by

$$\frac{\delta B}{B} = \frac{\delta \gamma}{\gamma} + \frac{\delta v}{v} - \frac{\delta R}{R}. \tag{12}$$

We obtain

$$\frac{\delta \gamma}{\gamma} = (\gamma^2 - 1)\frac{\delta v}{v}. \tag{13}$$

From the isochronous condition, the following equation should be fulfilled:

$$\frac{S + R\phi}{S + (R + \delta R)\phi} = \frac{v}{v + \delta v}. \tag{14}$$

Thus, we obtain

$$\frac{R\phi}{S + R\phi}\frac{\delta R}{R} = \frac{\delta v}{v}. \tag{15}$$

Inserting Eq. (13) and Eq. (15) into Eq. (12), the following equation is obtained:

$$\frac{\delta B}{B} = \left[\gamma^2 \frac{R\phi}{S + R\phi} - 1\right]\frac{\delta R}{R}. \tag{16}$$

Since the definition of the n-value is $n = -\frac{\delta B/B}{\delta R/R}$, the n-value to fulfill the isochronous condition is given by

$$n = 1 - \gamma^2 \frac{R\phi}{S + R\phi}. \tag{17}$$

In this case, the dispersion is given by

$$\xi = \frac{1}{\gamma^2}\frac{S + R\phi}{R\phi}R. \tag{18}$$

Since, in the rare-RI ring, the sector magnets used in TARN-II are reused, the edge angle is fixed to $+7.5$ deg. By using Eq. (10) with the present geometry of the rare-RI ring, the optimum edge angle to achieve the first-order isochronous field is $+2.95$ deg. Thus, if we introduce the n-value to achieve the first-order isochronous field, the n-value should be -0.59. There are some ways to introduce the n-value into the sector magnets. In the present design, we will introduce trim coils. We will use 10 trim coils. In preliminary calculations using 3D electromagnetic simulation software, TOSCA [14], after optimizing 10 trim coils so as to reproduce the ideal isochronous field, isochronicity with $\sim 2 \times 10^{-6}$ can be obtained for the radial direction with ± 50 mm, which covers the momentum acceptance of $\pm 0.5\%$. The lattice design of the ring is shown in Fig. 3. The dispersion and beta functions in the horizontal and vertical directions (β_x, β_y) are stable within $\xi = 6.50 \pm 0.25$ m, $\beta_x = 7.9 \pm 1.3$ m, $\beta_y = 11.6 \pm 0.6$ m throughout the ring. The horizontal and vertical tune values (Q_x, Q_y) are $Q_x = 1.25$, $Q_y = 0.82$, respectively.

The stability of the magnetic fields of the sector magnets is an important issue in the rare-RI ring. Preliminary measurements show that a definite correlation between the magnetic fields and the temperature of the yoke surface has been observed. A fluctuation in the temperature of the room causes a fluctuation in that of the yoke surface [15]. Thus, we need to take care of temperature control in the experimental room. In the cyclotron-like storage ring, the fluctuations of the magnetic fields in all sectors will be monitored by high-precision NMR ($\sim 10^{-7}$).

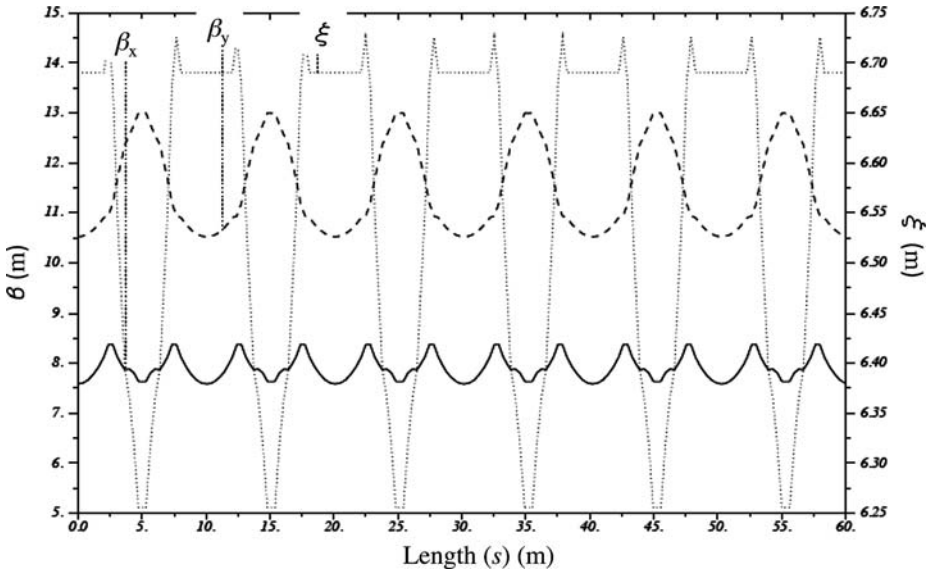

Fig. 3. Lattice design of the rare-RI ring. The solid line (broken line) shows the betatron function for x (y), respectively. The dotted line shows the dispersion (ξ).

3.2 Computer simulation

To examine the design of a cyclotron-like storage ring, and to evaluate the beam emittance with good isochronicity, we have developed a high-precision beam optics simulation [13]. To achieve as high a precision as possible, required for determining the beam particle trajectory, we adopt geometrical tracking in the magnetic sector under the assumption of a circular orbit within a given small spatial segment. For that purpose, it is sufficient that a magnetic sector is divided into 150 sub-sectors. In each sub-sector, the magnetic field is given as a function of the radial position, but is uniform around the vicinity of the beam trajectory. When the beam trajectory at the entrance of the sub-sector is given by (x, x', y, y', s), the four corresponding beam trajectories at the exit are evaluated successively in association with different B, as follows;

(i) evaluation of $(x_1, x_1', y_1, y_1', s_1)$ based on $B(x, s)$,
(ii) evaluation of $(x_2, x_2', y_2, y_2', s_2)$ based on $B(0.5(x + x_1), 0.5(s + s_1))$,
(iii) evaluation of $(x_3, x_3', y_3, y_3', s_3)$ based on $B(0.5(x + x_2), 0.5(s + s_2))$,
(iv) evaluation of $(x_4, x_4', y_4, y_4', s_4)$ based on $B(x_3, s_3)$.

Finally, the actual beam trajectory at the exit is given by taking a weighted mean of four evaluations:

$$x_{\text{exit}} = 1/6(x_1 + 2x_2 + 2x_3 + x_4), \tag{19}$$

$$x'_{\text{exit}} = 1/6(x_1' + 2x_2' + 2x_3' + x_4'), \tag{20}$$

$$y_{\text{exit}} = 1/6(y_1 + 2y_2 + 2y_3 + y_4), \tag{21}$$

$$y'_{\text{exit}} = 1/6(y_1' + 2y_2' + 2y_3' + y_4'). \tag{22}$$

$$s_{\text{exit}} = 1/6(s_1 + 2s_2 + 2s_3 + s_4) \tag{23}$$

The procedure entirely corresponds to a 4th-order Runge–Kutta algorithm. Finally, we have achieved a precision of 10^{-9} in $\delta T/T$ [13].

We performed a realistic simulation for the rare-RI ring by using the above simulation program. The resulting isochronicities on the x–x' plane are examined in view of a 2D contour map.

A typical 2D map for $\delta p/p = 0\%$ is shown in Fig. 4 for x. It is found that an emittance of $\sim 40\pi$ mm mrad for x is available under an isochronicity better than 10^{-6}.

3.3 *Injection beam-line*

The cyclotron-like storage ring is constructed in the K4 experimental room, downstream of the SHARAQ spectrometer. The rare RI is produced at the production target located at the entrance (F0) of BigRIPS [16]. The rare RI is transported to the ring via BigRIPS, the high-resolution beam-line [17], the SHARAQ spectrometer [18], and the newly constructed injection beam-line, and introduced into the ring through septum magnets and brought to the kicker magnet. It is noted that the results of early design work for the injection line are reported in Refs. [10,19]. We will newly construct an injection beam-line consisting of five quadrupole doublets and one dipole magnet. The quadrupole magnets are reused from those used in the main ring at the KEK proton synchrotron, which was shut down in 2007, and the dipole magnet is reused from that used as a magnetic field monitor in TARN-II. We need the dispersion matching condition for the injection of RI beams into the ring. The condition should be fulfilled at the position of the kicker magnet. A preliminary result of an ion-optical calculation by COSY [20] is shown in Fig. 5. Red, green, and blue lines correspond to particles with $\delta p/p = +0.5,\ 0.0,\ -0.5\%$, respectively. At F3, which is an achromatic focus, particle identification of RI is made and a trigger signal to the kicker magnet is produced. The momentum of a particle is measured at the dispersive focal plane, F5. A preliminary calculation by COSY shows that the angular acceptances for x and y are ± 15 mrad, respectively, and that the momentum acceptance is $\pm 0.5\%$ in the injection line. It is noted that these numbers are much smaller than those in BigRIPS. The angular acceptances of the BigRIPS separator have been designed to be 80 mrad horizontally and 100 mrad vertically, while the momentum acceptance is 6% [16]. To measure β of the rare RI, we will measure the time of flight (TOF) between F3 and

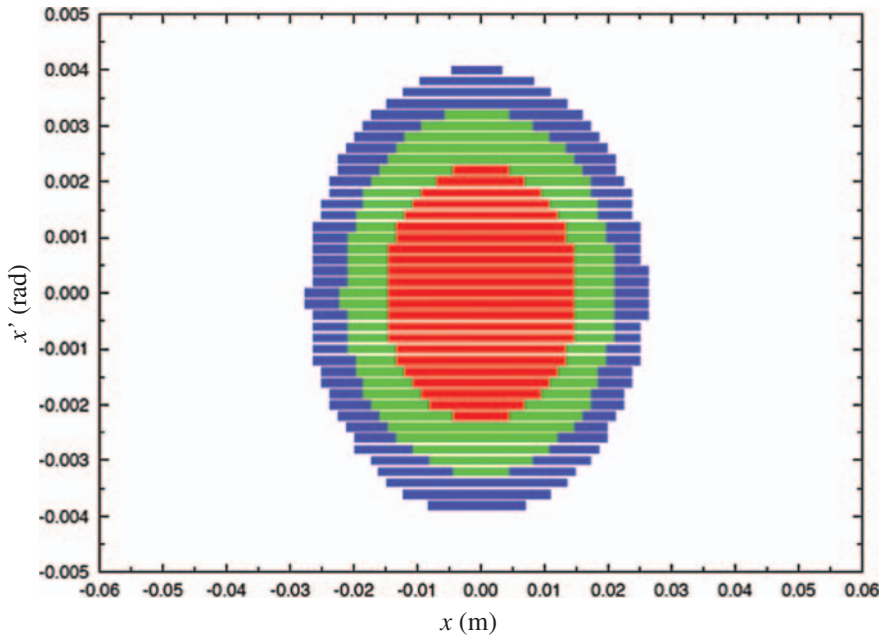

Fig. 4. Emittance for a good isochronicity region for x calculated by our simulation program. The red region shows the area where the isochronicity is $<10^{-6}$. The green and blue regions show the area where the isochronicity is $<2 \times 10^{-6}$ and $<3 \times 10^{-6}$, respectively. The results show the isochronicity after 2000 turns in the rare-RI ring.

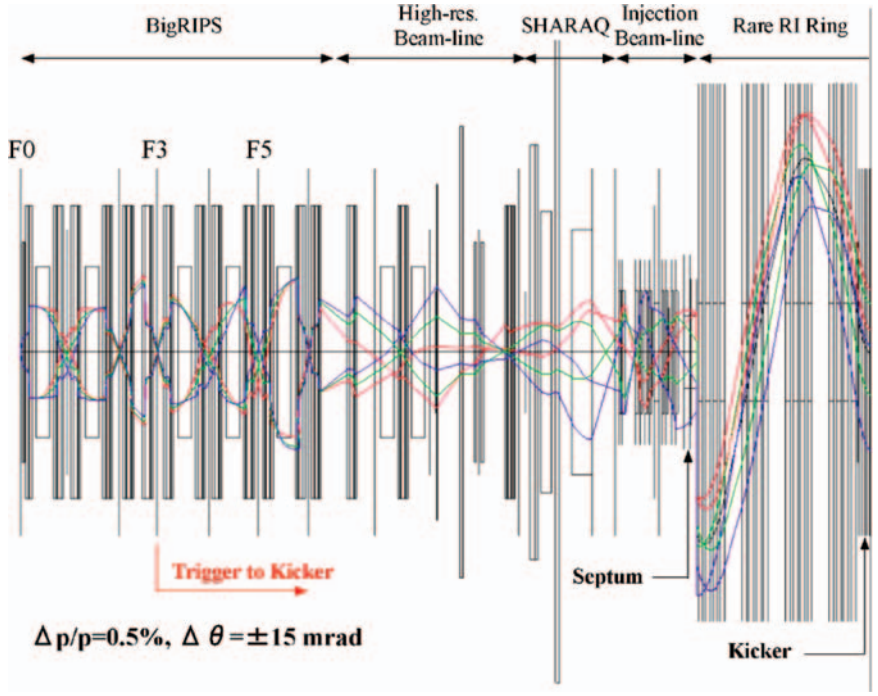

Fig. 5. Ion-optical calculation of the injection beam-line (from F0 in BigRIPS to the kicker magnets in the cyclotron-like storage ring). Red, green, and blue lines correspond to particles with $\delta p/p = +0.5$, 0.0, -0.5%, respectively.

the entrance of the septum magnet (ILC1 in Fig. 2). The flight time between them is 710 ns, which corresponds to $\sim 10^{-4}$ resolution if we achieve a 100 ps timing resolution. According to MOCADI simulations [21], higher-order aberrations for β can be corrected if we measure the momentum at F5 and the angular spread at F3.

3.4 Individual injection

Since the rare RI, which is produced by projectile-fragmentation or projectile-fission reactions of a primary beam from the cyclotron, arrives at the ring almost randomly in time, an individual RI injection mechanism [22] is needed for efficient use of the ring. Once the system is established, the injection efficiency will become 100% for any rare RI. When a particle passes through a trigger detector located at F3 of the BigRIPS, a trigger signal is generated. The distance between F3 and the kicker magnet is about 161 m, which corresponds to a flight time of about 945 ns for particles with 200 A MeV. The kicker magnet should be excited before the arrival of the beams. The trigger signal is transmitted to the kicker system by using a high-speed coaxial transmission cable, which can transfer the signal at 96% light velocity [23]. A possible path of the transmission cable is shown in Fig. 2, where the length of the cable is $\sim$100 m. A thyratron switch then immediately excites the kicker magnet before the particle arrives at the kicker magnet. To generate a high magnetic field with a rapid rise time ($\sim$100 ns) we will adopt a traveling-wave-type kicker magnet. In Table 2, the present possible delay times for the signal are shown. Recently, the development of an ultrafast-response kicker system has been successful, and thus a 275 ns delay time for the power-supply device for the thyratron has become available [24]. It is noted that a further shortening of the delay time ($\sim$50 ns) in the power-supply device would be possible. The development is ongoing.

Table 2. Delay time for individual injection in the rare-RI ring.

	Delay time (ns)
Trigger detector (plastic scintillator + PMT) at F3	50
Transmission cable from F3 to kicker magnet (∼100 m length)	350
Power-supply device for thyratron	275
Thyratron to flat-top center in kicker magnetic field	230
Total	905

4. Mass measurements in the rare-RI ring

4.1 Mass-measurement scheme

In the rare-RI ring, only one particle is injected by each individual injection. After injection, the particle circulates in the ring for about 2000 turns, which corresponds to about 0.7 ms in flight time. After 0.7 ms, the kicker is excited again, and ejects the particle. After ejection, the particle is identified again by some detectors. The particle identification (PID) procedure in the rare-RI ring is described in detail in Sect. 4.4. The resolution of circulation number (N) should be noted. By using Eq. (6), the following relation between a reference (isochronous) particle (0) and a non-isochronous particle (1) is obtained:

$$T_1 = \frac{\beta_0}{\beta_1} T_0. \tag{24}$$

We measure the total flight time (T_{tot}) in the cyclotron-like storage ring. For a non-isochronous particle, the circulation time is given by

$$T_1 = \frac{T_{\mathrm{tot}}}{N}. \tag{25}$$

By using Eq. (24) and Eq. (25), we obtain

$$N = \frac{T_{\mathrm{tot}}}{T_0} \frac{\beta_1}{\beta_0}. \tag{26}$$

Since we measure T_{tot} and T_0 with a resolution of $\sim 10^{-6}$ and β with $\sim 10^{-4}$, we obtain N with a resolution of $\sim 10^{-4}$. Thus, if the circulation number is about 2000, we can identify the exact value of the circulation number. Thus, we can obtain the circulation time (T_1) from the observed T_{tot}. The maximum injection rate in the rare-RI ring is limited by the kicker-magnet repetition rate, which is determined by ∼100 Hz in the present design; this is determined by the recharge time plus the recovery time of the thyratron. Thus, the maximum trigger rate in F3 should be less than 100 Hz.

4.2 Tuning and monitoring of the isochronous field

Tuning of the isochronous field is an important issue in mass measurements at the rare-RI ring. For tuning, we use *reference* particles. The reference particles should have a large momentum broadening (more than $\pm 0.5\%$) for tuning in the range of the momentum acceptance of the ring, $\delta p/p \sim \pm 0.5\%$. There are two possible candidates for reference nuclei; one is a primary beam at 200 A MeV and the other a secondary RI beam at 200 A MeV. The "primary" beam at 200 A MeV will be prepared by the accelerator itself in RIBF or by using energy degrader(s) in the beam-

line. In the latter case, to change the energy a little bit, we change the thickness of the energy absorber. Momentum selection can be done at a momentum dispersive focus, e.g. F5 in BigRIPS. Through a correlation between the beam momentum and the TOF in the storage ring, we can diagnose the isochronicity. When the measured isochronicity is worse than our requirement, we adjust the trim coils so that the time difference becomes $\sim 10^{-6}$.

Periodic monitoring of the isochronicity in the storage ring is an important issue. As mentioned in Sect. 3.1, we monitor the main magnetic field for each sector with an NMR probe with $\sim 10^{-7}$ accuracy. Another monitoring system is the RI beam itself. Injected RI beams are so-called 'cocktail beams'. We show an example of a cocktail beam in Fig. 6. Here, we assume the ^{78}Ni mass measurement. By using the LISE ++ simulation [25], ^{78}Ni is produced from U fission and is tuned to the central orbit in BigRIPS. According to this simulation, 12 nuclei other than ^{78}Ni are also injected into the rare-RI ring. Although the ^{78}Ni rate is pretty small ($\sim$1 event/day/pnA in the rare-RI ring), the ^{81}Ge and ^{82}Ge rates, which are closer to the stability line, are fairly high ($\sim$0.1 cps/pnA in the rare-RI ring). Since the masses of ^{81}Ge and ^{82}Ge are known with high accuracy ($\sim 3 \times 10^{-8}$) [2], ^{81}Ge and ^{82}Ge can act as the reference for the isochronous field periodically ($\sim$0.1 Hz).

4.3 *Feasibility of mass measurements*

The possible accessible area for mass measurements in the rare-RI ring is shown in Fig. 1. In the rare-RI ring, the mass of rare RI with a 1 event/day event rate can be measured with 10^{-6} accuracy. In Fig. 1, we estimate the event rate as follows. The expected production rates in BigRIPS are achieved in Ref. [26]. We take into account the transmission loss between BigRIPS and the rare-RI ring by considering the difference between the acceptances in BigRIPS and the injection line in the rare-RI ring. To estimate the transmission loss we used a MOCADI simulation [27]. For example, the transmission efficiency for ^{78}Ni produced by ^{238}U fission (^{86}Kr fragmentation) is 2.2% (6.6%), respectively. We used these numbers to estimate the rare-RI rate in the rare-RI ring. According to Fig. 1, the number of nuclei whose masses can be measured in the Rare-RI Ring is about 620 in total. For the region $Z < 50$, it is about 200. We expect quite big achievements in mass measurements in the rare-RI ring.

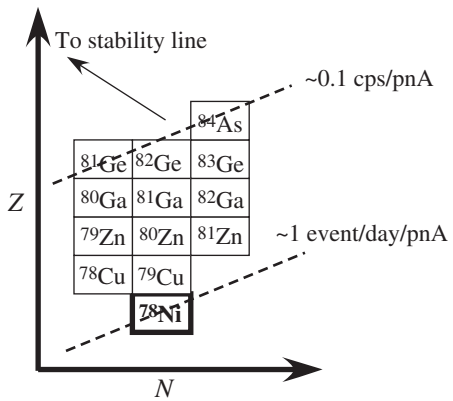

Fig. 6. Nuclear chart related to the ^{78}Ni mass measurement. The nuclei to be injected into the rare-RI ring accompanied by the ^{78}Ni beam are shown. Broken lines show the rate in the rare-RI ring. The calculation was done by using LISE++ [25].

4.4 Detectors

In order to achieve closed orbital distortion and the rough isochronous ion-optical condition in the rare-RI ring, charge pick-up detectors with a triangular shape will be installed at the entrance of each sector. These detectors can measure the timing and also the position information for the radial direction. We need at least 10^4 particles in one circulation to achieve position information with the detectors. To achieve a precise isochronous ion-optical condition, a sensitive Schottky pick-up system will be built and installed. With a standard Schottky pick-up, highly charged ions circulating in the ring induce mirror charges at each revolution on a couple of electrostatic pick-up electrodes located inside the ring aperture. Since the induced signals are periodic in time, a fast Fourier transform of the digitized signals from the pick-up yields the revolution frequency spectrum. The relative spread of the revolution frequency is proportional to that of the momentum of the circulating ions in the following:

$$\frac{\delta f}{f} = \eta \frac{\delta p}{p}, \tag{27}$$

where η is the frequency dispersion of the ring. Thus, the frequency spread allows us to tune the isochronous condition precisely to be as low as $\delta f/f \sim 10^{-6}$ if the pick-up has sufficient momentum and temporal resolving powers.

Due to the individual injection scheme, the number of the stored ions will reach only a few hundred, even for the primary beam. Therefore, a cavity-like resonant Schottky device must be developed. The resonant Schottky pick-up consists of a pillbox-type resonator and a ceramic gap connected with a vacuum beam pipe. The working frequency of the resonator will be a few hundred MHz, higher than the standard Schottky pick-up, which provides high sensitivity to stored single ions, excellent momentum separation, and fast temporal resolution. A similar device has successfully been installed and is in operation at the heavy-ion storage ring facility, ESR at GSI [28], and it is planned to be installed in CSRe at IMP.

For mass measurements in the rare-RI ring, a possible detector setup is shown in Fig. 7. Two time-of-flight (TOF) detectors are planned to be installed; they are placed at the entrance (ILC1 in Fig. 2) and exit (ILC2 in Fig. 2) of the ring. To determine the nuclear masses with a precision of 10^{-6}, the TOF should be measured with a precision of 10^{-6}. Since the flight time in the ring is 0.7 ms, the required time resolution turns out to be less than 100 ps. Thus, the required specifications for the TOF detectors are: i) to have good time resolution, better than 100 ps, ii) to have small

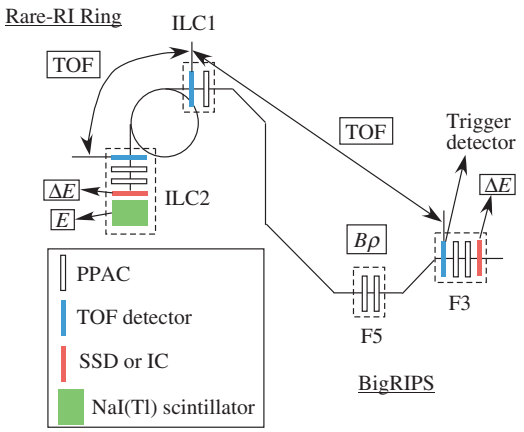

Fig. 7. Possible detector setup for mass measurements in the rare-RI ring. Observables measured by the detectors are shown by squares.

energy loss, iii) to make no change to the charge state by passing through a detector, and iv) to have a large effective area to match the beam size of 150×50 mm^2. A traditional plastic scintillator coupled with a photomultiplier tube can be used as TOF detectors for light nuclei, where the beam is fully ionized ($Z = q$) at 200 A MeV. We have tested the timing properties of several thin plastic scintillators (10–500 μm) designed for the rare-RI ring. The resultant timing resolutions reached a few tens of picoseconds [29]. On the other hand, for heavier nuclides, where charge divergence cannot be ignored by charge equilibrium in thick matter, a new detector consisting of a thin carbon foil with the detection of secondary electrons is preferred. The principle of this type of detector is that a beam generates secondary electrons in passing through a thin carbon foil. These electrons are transported to a micro-channel plate by crossed electric and magnetic fields [30]. This type of detector has already been applied for mass measurements in ESR [31] and CSRe [32]. However, the size of the C-foil is about 40mm ϕ for the detectors used in ESR and CSRe. Thus, we developed a large detector, where the size and thickness of the carbon foil are 100×50 mm^2 and 60 μg/cm^2. Currently, the observed time resolution is $\sigma \sim 130$ ps for a ∼300 A MeV ^{64}Ni beam and the observed efficiency is ∼56%.

Mention should be made of the detector setup for PID and corrections for β and TOF measurements. One of the merits of the rare-RI ring is the identification of particles and the monitoring of their trajectories during mass measurements. These cannot both be achieved in the present experiments at ESR and CSRe, because of the use of the fast extraction beam from the synchrotron. A possible detector setting for PID and beam tracking during mass measurements is shown in Fig. 7, where the TOF detectors to be used are mentioned above, Si solid-state detectors (SSD) or ion-chambers (IC) provide ΔE information, a Na I (Tl) scintillator provides E information, and parallel plate avalanche counters (PPAC) [33] provide position information, respectively. There is a constraint on the thickness of the detectors between F3 and ILC1 since we need to measure the TOF with 10^{-4} accuracy between them. Since the energy straggling produced by the detectors should be kept to less than 2×10^{-4} to maintain the time resolution of 10^{-4} from F3 to ILC1, the total thickness of the detectors between F3 and ILC1 should be less than 10 mg/cm^2 C equivalent, which corresponds to an effective thicknesses of 3 PPACs for RI beams with 200 A MeV. According to the GLOBAL code [25], fully ionized beams ($Z = q$) are dominant (>95%) for $Z < 40$ at 200 A MeV. Thus, for a beam with $Z < 40$, the traditional $B\rho$–TOF–ΔE measurements can provide complete particle identification. This should be done from F3 to ILC1, as shown in Fig. 7. According to Ref. [16], an A/q resolution of <0.03% for $A/q \sim 2.8$ is necessary to resolve q. The TOF resolution between F3 and ILC1 is expected to be $\sim 10^{-4}$, and the $B\rho$ resolution at F5 is also expected to be $\sim 10^{-4}$ since the dispersion of F5 is 3.3 cm/% in the standard optics [15]. Thus, complete identification including different q can be achieved from F3 to ILC1.

Additional PID can be performed from ILC1 to ILC2 by TOF–ΔE–E measurements. In this case, we can identify RI beams, except for knowing q. In this case, only the non-isochronous region (from ILC1 to the kicker magnet and from the kicker magnet to ILC2) contributes to the TOF measurements for PID. If we assume a 100 ps timing resolution for the TOF detectors, $\sim 10^{-4}$ TOF resolution can be obtained. Thus, in this case, the A resolution is determined by the E resolution. If we use a Na I (Tl) scintillator as the E detector, an E resolution of 0.18% can be obtained for the heavy ion beam [34]. Thus, we can also perform complete identification up to $A \sim 300$.

The trigger detector in F3 should be mentioned. This detector provides the start signal for the TOF measurement from F3 to ILC1 and also the trigger signal for the kicker magnet. If we use a standard plastic scintillator (∼100 μm thickness) with a photomultiplier as the detector, we can select its

pulse height for the detector. Since the pulse height corresponds to Z for RI beams, we can cut out unwanted particles and also provide rate adjustments for the kicker magnet. However, to achieve sufficient timing resolution ($\sim 10^{-4}$) between F3 and ILC1, a thickness of ~ 100 μm for the scintillator (~ 10 mg/cm^2 in C-equivalent) seems to be too large. We need to develop a detector with a smaller thickness and good Z or β selection, although the development is not trivial.

5. Other applications

We also consider other applications for the rare-RI ring, other than mass measurements. Lifetime measurements and reaction cross-section measurements in the ring are candidates. In the ESR, GSI, beta-decay half-life measurements have been successfully done by time-resolved SMS [35]. In particular, in the storage ring, beta-decay half-lives for highly charged states are measured. The dependence of the β-lifetimes on the atomic charge state of the parent ion has an obvious impact on our understanding of the processes ongoing in stellar nucleosynthesis [36]. For other applications, reaction studies with internal targets will be possible. We simply estimate the luminosity in the rare-RI ring as follows. To estimate the luminosity, we assume an ideal 10 μg/cm^2 hydrogen target, which corresponds to the thickness of the TOF counter in the ESR at GSI [31]. According to measurements at GSI, RI beams can circulate in the ring for $\sim 10^3$ turns in this case. In other words, the lifetimes of RI beams in the ring are ~ 1 ms in this case. Thus, the luminosity (L) is given by

$$L = f\, n\, i = 3 \times 10^{21} i(\mathrm{cm}^{-2}\,\mathrm{sec}^{-1}), \tag{28}$$

where f is the circulation number (s^{-1}), n is the number of target nuclei (cm^{-2}) and i is the RI beam intensity (cps). The luminosity will decrease monotonically when the beam intensity decreases. We can assume a more conservative setup, using a gas-jet as the internal target. The typical thickness of a hydrogen gas-jet is 3×10^{14} (cm^{-2}) [37]. However, the lifetime in the ring is more than 1 sec in this case. Thus, the luminosity is given by

$$L = 3 \times 10^{20} i(\mathrm{cm}^{-2}\,\mathrm{sec}^{-1}). \tag{29}$$

It is noted that, if the β-decay half-life is shorter than 1 sec, the luminosity is decreased from Eq. (29).

In the rare-RI ring, individual injection is applied. In individual injection, the maximum beam intensity is limited by the repetition rate of the kicker magnet. If we assume a 100 Hz repetition rate for the kicker magnet, the maximum luminosity goes up to 10^{23} cm^2 sec^{-1} in Eq. (29). For proton elastic scattering experiments on the beam-line, the typical target thickness is about 10 mg/cm^2 [38], which corresponds to a luminosity of 10^{23} cm^2 sec^{-1}. Thus, almost the same luminosity can be achieved in the ring with a much thinner target.

6. Summary

We have described the rare-RI ring at the RIKEN RI Beam Factory. The main purpose of the rare-RI ring is to measure the mass of rare RIs with 10^{-6} resolution based on isochronous mass spectrometry. For mass measurements of non-isochronous nuclei, measurement of β is essential, except for the circulation time measurement in the ring. The mass resolution for non-isochronous nuclei depends on the m/q difference. If we determine β with 10^{-4} resolution, we can achieve 10^{-6} mass resolution for nuclei with a 10^{-2} m/q difference. To realize isochronous mass spectrometry with 10^{-6} resolution for rare RIs, we will introduce two innovative pieces of apparatus. One is a cyclotron-like storage ring, which consists of 24 dipole magnets: 4 dipole magnets form

one sector and 6 sectors make up the ring. The ring has 6 straight sections and no focusing magnet. The dipole magnets to be used were originally used in a heavy-ion storage ring, TARN-II. The circumference of the ring is 60.35 m. We investigated the isochronous condition for a cyclotron-like storage ring. Since the dipole magnet has edge angles with $+7.5$ deg., the n-value should be -0.59 to achieve first-order isochronicity in the ring. To realize the n-value, we will set 10 trim coils in dipole magnets. For adjustments of higher-order isochronicity, the trim coils should be adjusted in detail. To evaluate the beam emittance with good isochronicity in the ring, we have developed a high-precision beam optics simulation. The simulation shows that an emittance of $\sim 40\ \pi$ mm mrad for x is available under an isochronicity of better than 10^{-6}. The cyclotron-like storage ring is located downstream of the SHARAQ spectrometer. We will newly construct an injection beam-line between the end of SHARAQ and the entrance of the ring. A preliminary calculation by COSY shows that the angular acceptances for x and y are ± 15 mrad, respectively, and that the momentum acceptance is $\pm 0.5\%$ in the injection line. Another innovative idea is individual injection, which is needed for 100% injection efficiency for rare RI. To realize individual injection, we developed an ultrafast-response kicker system, with which excitation of kicker magnets will be faster than the arrival of rare RIs with 200 A MeV.

We also described mass measurements in the rare-RI ring. After individual injection, the particle circulates in the ring for about 2000 turns, which corresponds to about 0.7 ms in flight time. We will measure the time-of-flight in the ring by two detectors located before and after the ring. We also show the feasibility of mass measurements in the rare-RI ring. By considering expected production rates in BigRIPS and the transmission loss between BigRIPS and the storage ring, it is found that for about 620 nuclei the mass can be measured. We are developing some detectors (resonant Schottky, TOF detectors with thin carbon foil, and so on) for mass measurements and tuning of the isochronous field in the storage ring. One of the merits of the rare-RI ring is the identification and monitoring of the particle during mass measurements. With a possible detector setup, particle identification can be made by $B\rho$–TOF–ΔE before injection and by TOF–ΔE–E after ejection, respectively. Other than mass measurements, the rare-RI ring has some potential for other applications. In the ESR, GSI, beta-decay half-life measurements have been successfully done by time-resolved Schottky mass spectrometry. In the rare-RI ring, lifetime measurements and reaction cross-section measurements will be possible. Reaction studies of rare RIs with an internal target is one attractive application, and it will be possible to achieve almost the same luminosity in the measurements in the rare-RI ring as in fixed-target experiments, but with a thinner target.

References

[1] H. Koura et al., Prog. Theor. Phys. **113**, 305 (2005).
[2] http://amdc.in2p3.fr/masstables/Ame2011int/filel.html.
[3] T. Ohnishi et al., J. Phys. Soc. Jpn. **77**, 083201 (2010).
[4] T. Ohnishi et al., J. Phys. Soc. Jpn. **79**, 073201 (2010).
[5] J. J. Cowan, F.-K. Thielemann, and J. W. Truran, Phys. Rep. **208** 267 (1991).
[6] D. Lunny, J. M. Pearson, and C. Thibault, Rev. Mod. Phys. **75**, 1021 (2003).
[7] K. Blaum, Phys. Rep. **425**, 1 (2006).
[8] B. Franzke, H. Geissel, and G. Meunzenberg, Mass. Spec. Rev. **27**, 428 (2008).
[9] T. Yamaguchi et al., Proceedings of the 6th International Conference on Nuclear Physics at Storage Rings STORI'05, Schriften des Forschungszentrums Julich, Matter and Materials, Volume 30, 2005, p.297.
[10] Y. Yamaguchi et al., Nucl. Instrum. Methods Phys. Res., Sect. B **266**, 4575 (2008).
[11] Y. Yasuda et al., Int. J. Mod. Phys. E **18**, 459 (2009).
[12] T. Katayama et al., Part. Accel. **32**, 105 (1990).

[13] I. Arai et al., Int. J. Mod. Phys. E **18**, 498 (2009).
[14] http://www.vectorfields.co.uk/
[15] Y. Yasuda et al., RIKEN Accel. Prog. Rep. **42**, 197 (2009).
[16] T. Kubo et al., Nucl. Instrum. Methods Phys. Res., Sect. B **204**, 97 (2003).
[17] T. Kawabata et al., Nucl. Instrum. Methods Phys. Res., Sect. B **266**, 4201 (2008).
[18] T. Uesaka et al., Nucl. Instrum. Methods Phys. Res., Sect. B **266**, 4218 (2008).
[19] K. Makino and M. Berz, Nucl. Instrum. Nucl. Instrum. Meth A **558**, 346 (2005).
[20] M. Yamaguchi et al., Proceedings of the 6th International Conference on Nuclear Physics at Storage Rings STORI'05, Schriften des Forschungszentrums Julich, Matter and Materials, Volume 30, 2005, p.315.
[21] N. Iwasa et al., Nucl. Instrum. Methods Phys. Res., Sect. B **126**, 284 (1997).
[22] I. Meshkov et al., Nucl. Instrum. Methods Phys. Res., Sect. A **523**, 262 (2004).
[23] HITACHI high frequency coaxial transmission cables, HITACHI Cable, Ltd.
[24] Y. Yamaguchi et al., RIKEN Accel. Prog. Rep. **44**, 157 (2011).
[25] http://lise.nscl.msu.edu/lise.html
[26] Estimated RI beam intensities in http://www.nishina.riken.jp/RIBF/BigRIPS/intensity.html
[27] N. Iwasa et al., Nucl. Instrum. Methods Phys. Res., Sect. B **126**, 284 (1997).
[28] F. Nolden et al., Nucl. Instrum. Methods Phys. Res., Sect. A **659**, 69 (2011).
[29] S. Nakajima et al., Nucl. Instrum. Methods Phys. Res., Sect. B **266**, 4621 (2008).
[30] J. D. Bowman and R. H. Heffner, Nucl. Instrum. Methods **148**, 503 (1978).
[31] M. Hausmann et al., Hyperfine Int. **132**, 291 (2001).
[32] B. Mei et al., Nucl. Instrum. Methods Phys. Res., Sect. A **624**, 109 (2010).
[33] H. Kumagai et al., Nucl. Instrum. Methods Phys. Res., Sect. A **470**, 562 (2001).
[34] T. Suda et al., *2005 Annual Report of the Research Project with Heavy Ions at NIRS-HIMAC* (2006) p. 181.
[35] Yu. A. Litvinov et al., Nucl. Phys. A **756**, 3 (2005).
[36] K. Takahashi and K. Yokoi, Nucl. Phys. A **404**, 578 (1983).
[37] D. Allspach et al., Nucl. Instrum. Methods Phys. Res., Sect. A **410**, 195 (1998).
[38] Y. Matsuda et al., RIKEN Accel. Prog. Rep. **43**, 25 (2010).